

Electronic supplementary information

1. Experimental

1.1. Catalyst preparation procedure

The general procedure of preparation was divided in two steps to separate nucleation and growth processes. In a first step, Pd nanoparticles (NPs) of 3-4 nm in diameter were obtained using a strong reducing agent, sodium borohydride (NaBH₄). In a second step, these Pd “seeds” were injected in a growth solution to control the formation of Pd nanocrystals.

Synthesis of Pd nanoparticle seeds. Isotropic palladium NP were prepared as follows : 50 mL of an aqueous 0.5 mM Na₂PdCl₄ solution was mixed with 25 mL of an aqueous 0.3 M cetyltrimethylammonium bromide (CTAB) solution prepared at 303 K. Next, 6 mL of an ice-cold aqueous 0.01 M NaBH₄ solution was added quickly under vigorous stirring. The solution turned dark immediately after the borohydride addition. The seed solution was used 2 h after its preparation.

Synthesis of the S#2 catalyst. The growth solution was obtained by mixing 50 mL of an aqueous 1.0 mM Na₂PdCl₄ solution with 50 mL of an aqueous 0.08 M CTAB solution under gently stirring at 303 K. After 5 min of mixing, a turbid solution formed, indicating the formation of a CTAB-Pd complex. 0.7 mL of an aqueous 0.08 M sodium ascorbate solution was then added. Finally, 120 μL of the seed solution was injected. The initial orange red solution changed progressively in 30 min into a dark solution indicating the reduction of the metallic precursor. After 48 h of aging, the solution was centrifuged at 3000 rpm for 45 min to reduce the volume from 200 mL to 2 mL. This concentrated solution was impregnated onto 5 g of α-Al₂O₃ (S_{BET} = 8 m² g⁻¹, V_p = 0.52 cm³ g⁻¹). After maturation for 24 h at 303 K, the solid was washed with ethanol to remove the CTAB surfactant and dried 48 h at 303 K.

Synthesis of S#1 and S#3 catalysts. The procedures were similar to that for the S#2 catalyst, except the use of a higher temperature (333 K) for S#1, and an immediate injection of sodium ascorbate without waiting for the CTAB-Pd complex for S#3.

See also: Berhault *et al.*, *J. Phys. Chem. C*, 2007, **111**, 5915.

1.2. Experimental setup for catalytic characterization

The setup is composed of an ultra-high vacuum (UHV) preparation chamber coupled to a static reaction cell, dedicated to catalytic testing of low-surface-area catalysts (mainly single-crystals or powders). Samples are transferred from the preparation chamber to the cell via an intermediate UHV chamber, which is also used for gas evacuation by independent turbomolecular pumping. The cell is fully UHV-compatible and can operate at gas pressures up to 1 atm. It is a compact (120 cm³) cylindrical stainless-steel chamber equipped with a glass viewport, a K-type thermocouple (isolated in a stainless steel jacket) pointing near to the sample surface, a sample holder and a full-metal injection valve. Powder catalysts are held in

small stainless-steel “stubs” that allow their manipulation from outside. They can be outgassed (up to ~1500 K) in the preparation chamber using a halogen lamp. The reactor, which is separated from the transfer chamber by a Viton™-seal gate valve, can be externally heated to ~500 K. Reactive gas mixtures are prepared in a separate turbo-pumped chamber containing two complementary capacitance diaphragm gauges (pressure range 10⁻³-10³ Torr) and several gas entries. In the course of a reaction, a small amount of the mixture is continuously extracted from the reactor through a leak valve, and analyzed by a quadrupole mass spectrometer (QMS) evacuated by a diffusion pump coupled to a liquid nitrogen trap.

1,3-butadiene (N2.6 purity), hydrogen (N6.0) and argon (N5.7) were supplied by Air Liquide™. The reaction kinetics was followed by analyzing mass spectrometry peaks 40, 54, 56 and 58, which correspond to the masses of Ar, C₄H₆ (butadiene), C₄H₈ (butenes) and C₄H₁₀ (butane) molecules, respectively. It must be noticed that the three isomers of butene were not distinguished with mass spectrometry. After normalization by the Ar signal, the data were corrected for ion fragmentation and spectrometer sensitivity to obtain partial pressures.

Repeated reaction cycles, each cycle including injection of the reactants, reaction run, and evacuation of the reacted gases by turbomolecular pumping, were performed in order to investigate the stability of the catalysts.

2. Analysis of TEM micrographs

2.1. Size histograms

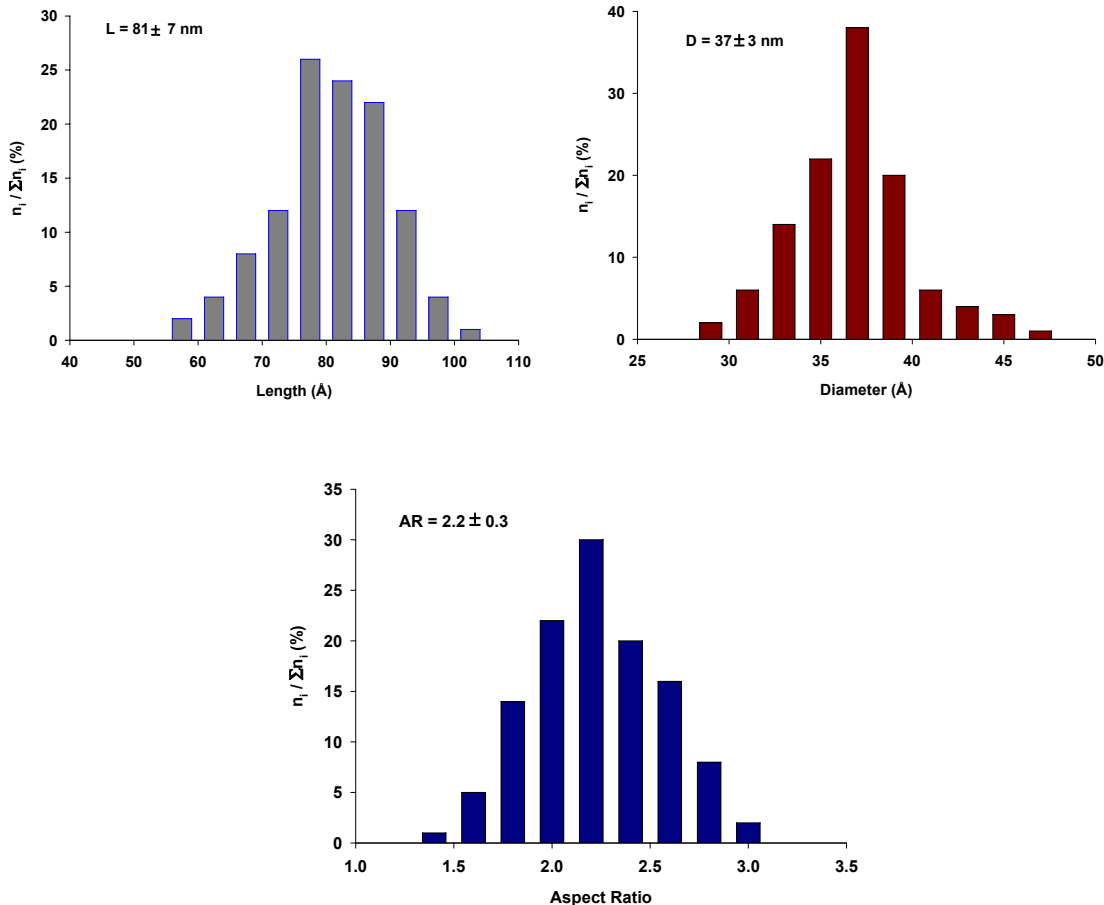


Fig. S1 Size distribution of elongated prismatic particles: length (L), diameter (D) and aspect ratio (AR=L/D) (S#1 catalyst).

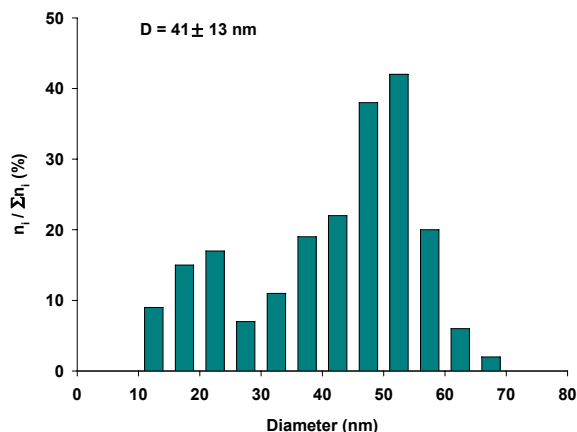


Fig. S2 Size distribution of icosahedric particles (S#2 catalyst). The presence of a bimodal distribution results from the thermodynamically-controlled growth regime of icosahedric particles combined with Ostwald ripening consuming the smallest particles in favour of the biggest ones.

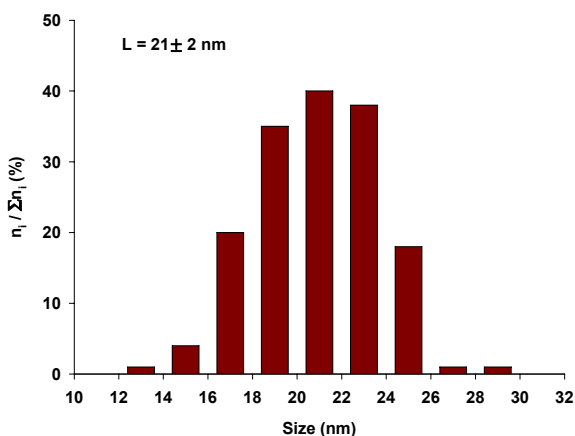


Fig. S3 Size distribution of cubic particles (S#3 catalyst).

2.2. Particle morphology and TOF calculation

Each sample is characterized by particular shapes, as indicated in Table 1. These shapes were determined by statistical analysis of TEM images (as those of Fig. 1). To each shape corresponds a series of facets of defined orientation [mainly (111) or (100)], leading to a particular *morphology* (shape and crystallographic nature of the facets). The morphological analysis is facilitated by the abundant literature (see e.g. Refs. 1-5 and 8) focusing on the atomic structure of fcc nanoparticles. Thus, through geometric modelling of each type of particle (cubes, icosahedra, prisms [Fig. S4], etc.), and weighting by the fraction of each morphology in the sample (see Table 1, 2nd column), we could determine the surface fraction of (111) facets and the dispersion (both collected in Table 1) for each sample. Formulas are given below.

The TOF were calculated according to the equation:

$$TOF = \frac{V}{m_{Pd} d_{Pd} kT} \frac{dP_{C_4H_6}}{dt} (t = 0)$$

where V is the reactor volume (120 cm³), m_{Pd} the mass of metal in the catalyst (100 mg × Pd loading), k the Boltzmann constant, T the temperature and P_{C₄H₆}(t) the partial pressure of butadiene.

The metallic dispersion (surface atoms / total number of atoms) was calculated as follows:

$$d_{Pd} = \frac{\sum_i x_i N_i^{surf}}{\sum_i x_i N_i^{tot}}$$

where x_i is the number of particles of type i (corresponding to a particular morphology), N_i^{surf} the number of surface Pd atoms in particles of type i and N_i^{tot} the total number of Pd atoms in particles of type i. x_i, N_i^{surf} and N_i^{tot} were derived from TEM analysis and geometric modelling of the particles (a mean size was used for each type).

Similarly, the surface fraction of (111) facets is given by:

$$f_{(111)} = \frac{\sum_i x_i N_i^{(111)}}{\sum_i x_i N_i^{surf}}$$

where N_i⁽¹¹¹⁾ is the number Pd(111) atoms in particles of type i.

To the best of our knowledge, the synthesis of prismatic particles, showing mostly (111) facets, had never been reported for palladium. However, such a shape has already been discussed in the literature [M.P. Pileni, *J. Phys. Chem. C*, 2007, **111**, 9019]. Figure S4 describes this type of particle.

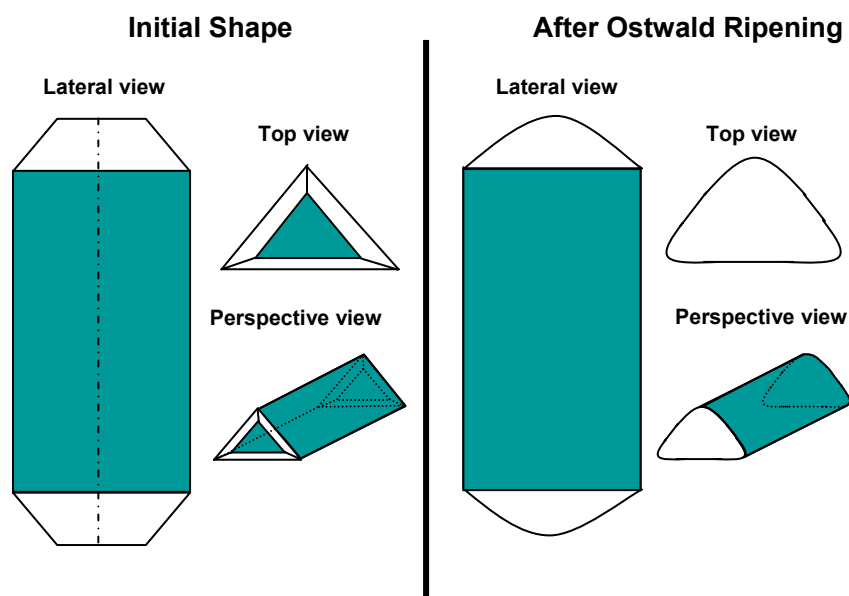


Fig. S4 Scheme of a nanoprism (S#1 catalyst). (111) facets are coloured. After the preparation process, elongated particles are rounded at both ends (right side). Lateral (111) facets constitute ~80% of their total surface area.

3. Additional experiments

3.1. ICP and XPS analysis

Due to the use of Na₂PdCl₄ (precursor), NaBH₄ (reductant) and C₁₉H₄₂NBr (CTAB surfactant) in the synthesis procedure, the following elements were dosed by ICP: Pd, B, Br, Cl, Na, N, Si (common support impurity) and C (common surface impurity). Less than 10 wt.ppm (detection limit) of Br and Cl were detected. Si and Na were detected both by ICP (up to 3.6 and 0.5 wt.%, respectively, for a S#2-type sample) and XPS, since they are major impurities of the α-Al₂O₃ support. Only C was also detected by XPS, but no trace of B or N was found, although the atomic sensitivity factors are of the same order (0.13, 0.25 and 0.42 for B, C and N, respectively [<http://www.uksaf.org/data/sfactors.html>]).

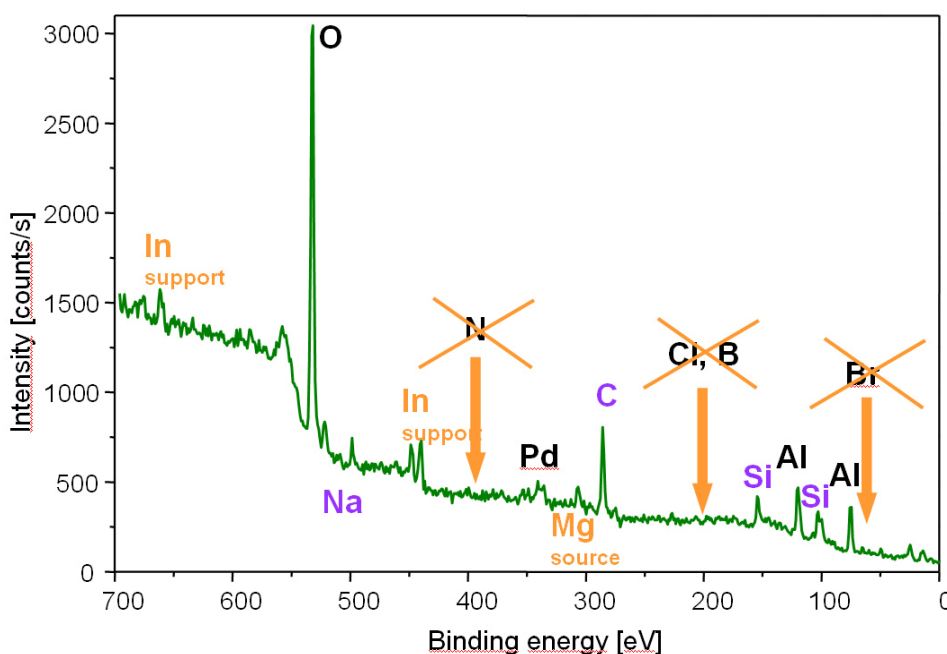


Fig. S5 XPS spectrum (general scan, Al-K α radiation) for a S#2-type sample.

3.2. Thermodesorption spectroscopy

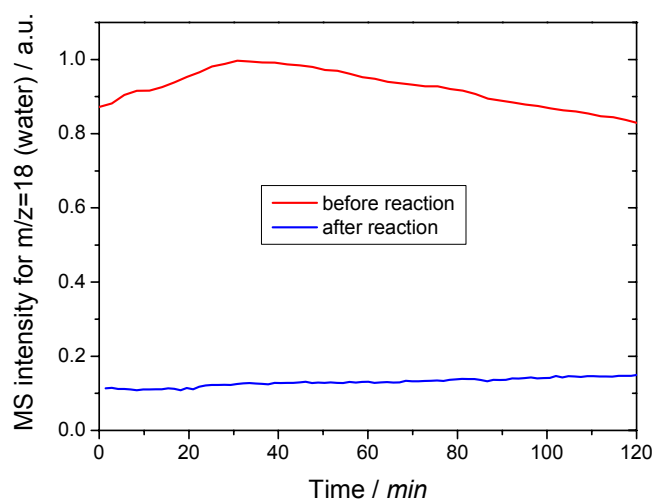


Fig. S6 A S#2-type sample was slowly heated to 330 K under ultrahigh vacuum while mass spectrometer signals were recorded for $m/z=1-100$. Water (and water only, $m/z=18$ and 17) is desorbed, especially before reaction (butadiene hydrogenation at room temperature) on the fresh Pd/Al₂O₃ catalyst (9 mg). This may explain why the catalyst is activated by heating to ~350 K (Fig. 2a of the article).

3.3. Transmission electron microscopy after sample heating

Above ~400 K, an aggregation phenomenon is observed, leading to the junction of different nanocrystals together and to the consumption of the most reactive facets. An example of such a process is presented in Figure S7 for a temperature of 423 K. In this example, a plate-like particle with a 2D triangular aspect fused with a nanorod. Each of these particles tend to consume its most reactive facets [(110) or (100) edge facets for the triangular particle, (100) lateral facets for the nanorod]. This process led to an increase of the relative proportion of the most thermodynamically stable (111) planes. However, all of the particles fusing with each other kept their initial morphology.

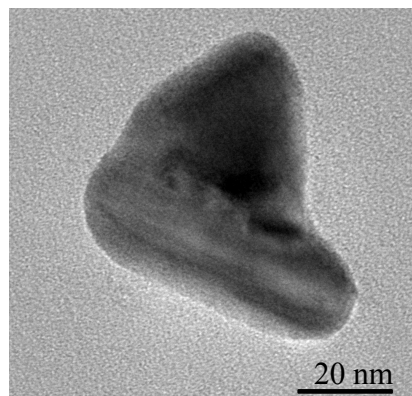


Fig. S7 TEM of two aggregated Pd particles fusing together. The sample preparation was similar to that reported for the S#2 catalyst, but it was additionally pretreated under flowing

H₂ at 423 K for 2 hours. The probability of coalescence increases with the pretreatment temperature.